Cluster Construction by Reactions of an Isomeric Pair of Trinuclear Clusters Containing a Tetrathiotungstate Fragment, [{Cp′Ru(CO)}$_2${W(μ-S)$_4$}] and [{Cp′Ru(CO)}$_2${W(=S)(μ_3-S)(μ-S)$_2$}] (Cp′ = η^5-C$_5$Me$_5$, η^5-C$_5$Me$_4$Et), with Platinum Complexes

Masahiro Yuki, Masaaki Okazaki, and Hiroshi Ogino*

Department of Chemistry, Graduate School of Science, Tohoku University, Sendai 980-8578, Japan

Received November 20, 2000

The reactions of the isomeric pair of trinuclear clusters [{Cp′Ru(CO)}$_2${W(μ-S)$_4$}] (**3**) and [{Cp′Ru(CO)}$_2${W(=S)(μ_3-S)(μ-S)$_2$}] (**4**) with 1 equiv of [PtMe$_2$(cod)] gave the respective tetranuclear clusters [{Cp′Ru(CO)}$_2${W(μ_3-S)$_2$(μ-S)$_2$}(PtMe$_2$)] (**5**) and [{Cp′Ru(CO)}$_2${W(=S)-(μ_3-S)$_3$}(PtMe$_2$)] (**6**) (Cp′ = η^5-C$_5$Me$_5$ (=Cp*), η^5-C$_5$Me$_4$Et) containing a tetrathiotungstate fragment as the main products, which corresponds to an isomeric pair. The pentanuclear cluster [{Cp′Ru(CO)}$_2${W(μ_3-S)$_4$}(PtMe$_2$)$_2$] (**7**) was obtained by the reaction of [{Cp′Ru(CO)}$_2$-{W(μ-S)$_4$}] (**3**) with 2 equiv of [PtMe$_2$(cod)]. Treatment of [{Cp*Ru(CO)}$_2${W(μ_3-S)$_2$(μ-S)$_2$}-(PtMe$_2$)] (**5a**) with excess HCl underwent monochlorination of the methyl ligand in the PtMe$_2$ moiety to give [{Cp*Ru(CO)}$_2${W(μ_3-S)$_2$(μ-S)$_2$}(PtClMe)] (**8**) selectively. In the reaction of [{Cp*Ru(CO)}$_2${W(μ_3-S)$_4$}(PtMe$_2$)$_2$] (**7a**) with 1 equiv of HCl, monochlorination at one platinum center took place to give [{Cp*Ru(CO)}$_2${W(μ_3-S)$_4$}(PtClMe)(PtMe$_2$)] (**10**) quantitatively, whereas the reaction of **7a** with excess HCl took place with monochlorination at each platinum center to give [{Cp*Ru(CO)}$_2${W(μ_3-S)$_4$}(PtClMe)$_2$] (**9**). The trinuclear cluster [{Cp′Ru(CO)}$_2${W(μ-S)$_4$}] (**3**) reacted with the platinum(0) complex [Pt(C$_2$H$_4$)(PPh$_3$)$_2$] to give the novel pentanuclear cluster [{Cp′Ru(CO)}(WS$_4$)(Cp′Ru){Pt$_2$(PPh$_3$)$_2$(μ-CO)}] (**11**). The product **11** has a new platinum−platinum bond bridged by a carbonyl ligand which is originally located on a ruthenium center. The tetrathiotungstate ligand in **11** bridges the ruthenium fragment Cp′Ru(CO) and the three-membered metallacycle (Cp′Ru){Pt(PPh$_3$)}$_2$-(μ-CO).

Introduction

Transition metal−sulfur clusters have attracted considerable attention due to the possible relevance to the active sites of metalloenzymes[1] and hydrodesulfurization catalysts.[2] A large number of synthetic and structural studies on transition metal−sulfur clusters have been explored; however, systematic methods of cluster construction have not been well established.[3] Stepwise aggregation of small metal units would be a promising method to build up a wide variety of clusters. A series of dinuclear transition metal−sulfur complexes of the type [Cp$^{\#}{}_2$M$_2$S$_4$] (Cp$^{\#}$ = substituted and nonsubstituted cyclopentadienyls) have been used as the precursors for not only homometallic but also heterometallic clusters.[4] Some cubane-type clusters were synthesized by the reactions of [Cp$^{\#}{}_2$M$_2$S$_4$] with the appropriate metal complexes. The iron dimer [Cp*$_2$Fe$_2$S$_4$] (Cp* = η^5-C$_5$-Me$_5$) reacted with 2 equiv of [Cp*Ru(NCMe)$_3$](PF$_6$) to give the cationic cubane-type cluster [Cp*$_4$Fe$_2$Ru$_2$S$_4$]-(PF$_6$)$_2$.[4a] Photolysis of the molybdenum dimer [Cp*$_2$-Mo$_2$S$_4$] and [Fe(CO)$_5$] afforded the cubane-type cluster [(Cp*Mo)$_2${Fe(CO)$_2$}$_2$(μ_3-S)$_4$] and the trinuclear cluster [(Cp*Mo)$_2$(μ-S$_2$)(μ_3-S)$_2${Fe(CO)$_2$}].[4b] The molybdenum dimer also reacted with [Co$_2$(CO)$_8$] under the thermal conditions to give the Mo$_2$Co$_2$S$_4$ cubane-type cluster [(Cp*Mo)$_2${Co(CO)}$_2$(μ_3-S)$_4$].[4c] In previous papers, we reported the formation of an isomeric pair of tetranuclear clusters **1** and **2** by the reaction of the ruthenium dimer [Cp*$_2$Ru$_2$S$_4$] with [W(CO)$_3$(NCMe)$_3$] (Scheme 1).[5] Elemental analysis and mass spectral data of the products established the formula as Cp*$_2$Ru$_2$W$_2$S$_4$(CO)$_6$,

(1) Holm, R. *Adv. Inorg. Chem.* **1992**, *38*, 1.
(2) (a) Wiegand, B. C.; Friend, C. M. *Chem. Rev.* **1992**, *92*, 491. (b) Mansour, M. A.; Curtis, M. D.; Kampf, J. W. *Organometallics* **1997**, *16*, 3363. (c) Curtis, M. D.; Druker, S. H. *J. Am. Chem. Soc.* **1997**, *119*, 1027.
(3) (a) Ogino, H.; Inomata, S.; Tobita, H. *Chem. Rev.* **1998**, *98*, 2093. (b) Gladfelter, W. L.; Geoffroy, G. L. *Adv. Organomet. Chem.* **1980**, *18*, 207. (c) Roberts, D. A.; Geoffroy, G. L. In *Comprehensive Organometallic Chemistry*; Abel, E. W., Stone, F. G. A., Wilkinson, G., Eds.; Pergamon Press: Oxford U.K., 1982; Vol. 6, Chapter 40.
(4) (a) Feng, Q.; Rauchfuss, T. B.; Wilson, S. R. *J. Am. Chem. Soc.* **1995**, *117*, 4702. (b) Brunner, H.; Janietz, N.; Wachter, J.; Zahn, T.; Ziegler, M. L. *Angew. Chem., Int. Ed. Engl.* **1985**, *24*, 133. (c) Brunner, H.; Wachter, J. *J. Organomet. Chem.* **1982**, *240*, C41. (d) Mitsui, T.; Inomata, S.; Ogino, H. *Inorg. Chem.* **1994**, *33*, 4934. (e) Yuki, M.; Kuge, K.; Okazaki, M.; Mitsui, T.; Inomata, S.; Tobita, H.; Ogino, H. *Inorg. Chim. Acta* **1999**, *291*, 395. (f) Okazaki, M.; Yuki, M.; Kuge, K.; Ogino, H. *Coord. Chem. Rev.* **2000**, *198*, 367. (g) Houser, E. J.; Krautscheid, H.; Rauchfuss, T. B.; Wilson, S. R. *J. Chem. Soc., Chem. Commun.* **1994**, 1283. (h) Bolinger, C. M.; Weatherill, T. D.; Rauchfuss, T. B.; Rheingold, A. L.; Day, C. S.; Wilson, S. R. *Inorg. Chem.* **1986**, *25*, 634. (i) Veturelli, A.; Rauchfuss, T. B.; Verma, A. K. *Inorg. Chem.* **1997**, *36*, 1360.

10.1021/om000985t CCC: $20.00
Publication on Web 04/04/2001

Scheme 1. Formation Pathway of 1 and 2

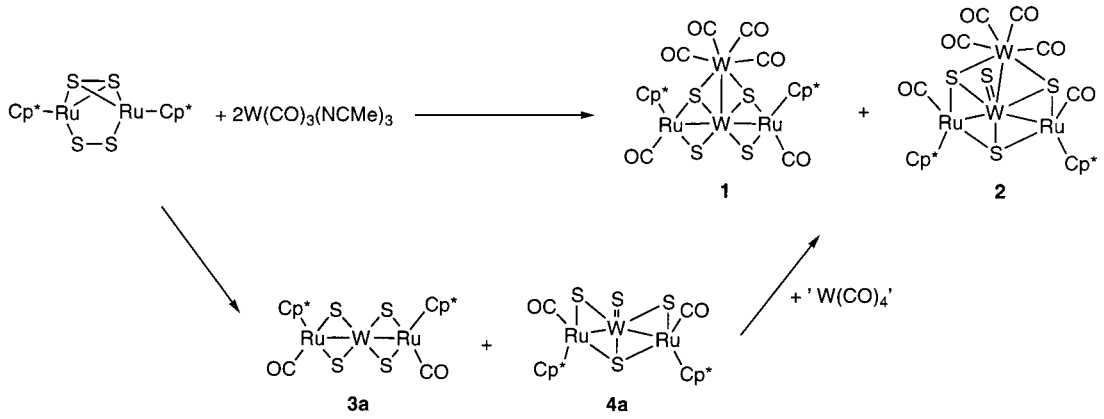

which is consistent with formation of the cubane-type metal−sulfur cluster $[(Cp^*Ru)_2\{W(CO)_3\}_2(\mu_3\text{-}S)_4]$. However, the X-ray structure analysis revealed that this is not the case. Clusters **1** and **2** are tetrathiotungstate clusters in which the tetrathiotungstate moiety bridges two ruthenium Cp*Ru(CO) fragments and one tungsten $W(CO)_4$ fragment, as illustrated in Scheme 1. Moreover, the isomeric pair of trinuclear clusters **3a** and **4a** was also isolated and considered as the intermediates for the formation of **1** and **2**, because tetranuclear clusters **1** and **2** were formed by the reactions of trinuclear clusters **3a** and **4a** with $[W(CO)_3(NCMe)_3]$ and CO. These results imply that trinuclear clusters **3a** and **4a** are useful building blocks for cluster construction. We report here cluster expansion by the reactions of the trinuclear clusters $[\{Cp'Ru(CO)\}_2\{W(\mu\text{-}S)_4\}]$ (**3a**, Cp′ = Cp*; **3b**, Cp′ = η^5-C_5Me_4Et) and $[\{Cp'Ru(CO)\}_2\{W(=S)(\mu_3\text{-}S)(\mu\text{-}S)_2\}]$ (**4a**, Cp′ = Cp*; **4b**, Cp′ = η^5-C_5Me_4Et) with $[PtMe_2(cod)]$ and $[Pt(C_2H_4)(PPh_3)_2]$ to produce Ru_2PtWS_4 and $Ru_2Pt_2WS_4$ clusters, which are characterized by the spectroscopic data and X-ray crystal structure analysis. Part of this work has been previously reported in a preliminary form.[6]

Results and Discussion

Reactions of 3 and 4 with [PtMe$_2$(cod)]. The reaction of $[\{Cp^*Ru(CO)\}_2\{W(\mu\text{-}S)_4\}]$ (**3a**) with 1 equiv of the platinum(II) complex $[PtMe_2(cod)]$ at 80 °C for 18 h afforded three kinds of new clusters: $[\{Cp^*Ru(CO)\}_2\{W(\mu_3\text{-}S)_2(\mu\text{-}S)_2\}(PtMe_2)]$ (**5a**), $[\{Cp^*Ru(CO)\}_2\{W(=S)(\mu_3\text{-}S)_3\}(PtMe_2)]$ (**6a**), and $[\{Cp^*Ru(CO)\}_2\{W(\mu_3\text{-}S)_4\}(PtMe_2)_2]$ (**7a**) (eq 1). The terminal sulfide cluster **6a**, which is the geometric isomer of **5a**, was obtained by the reaction of the terminal sulfide cluster $[\{Cp^*Ru(CO)\}_2\{W(=S)(\mu_3\text{-}S)(\mu\text{-}S)_2\}]$ (**4a**) with $[PtMe_2(cod)]$ as a major product (eq 2). Treatment of the isolated **5a** with 1 equiv of $[PtMe_2(cod)]$ in benzene-d_6 at 80 °C for 11 h led to the formation of **7a** in 60% conversion yield (eq 3). Furthermore, thermal reaction of **3a** with 2 equiv of $[PtMe_2(cod)]$ under the same conditions as those of eq 1 gave **7a** as a major product (eq 4). These results indicate that the mono-$PtMe_2$ cluster **5a** is an intermediate for the formation of the bis-$PtMe_2$ cluster **7a**. The C_5Me_4Et derivatives $[\{(\eta^5\text{-}C_5Me_4Et)Ru(CO)\}_2\{W(\mu_3\text{-}S)_2(\mu\text{-}S)_2\}(PtMe_2)]$ (**5b**), $[\{(\eta^5\text{-}C_5Me_4Et)Ru(CO)\}_2\{W(=S)(\mu_3\text{-}S)_3\}(PtMe_2)]$ (**6b**), and $[\{(\eta^5\text{-}C_5Me_4Et)Ru(CO)\}_2\{W(\mu_3\text{-}S)_4\}(PtMe_2)_2]$ (**7b**) were also obtained from $[\{(\eta^5\text{-}C_5Me_4Et)Ru(CO)\}_2\{W(\mu\text{-}S)_4\}]$ (**3b**) and $[\{(\eta^5\text{-}C_5Me_4Et)Ru(CO)\}_2\{W(=S)(\mu_3\text{-}S)(\mu\text{-}S)_2\}]$ (**4b**) by reactions similar to eqs 2 and 4.

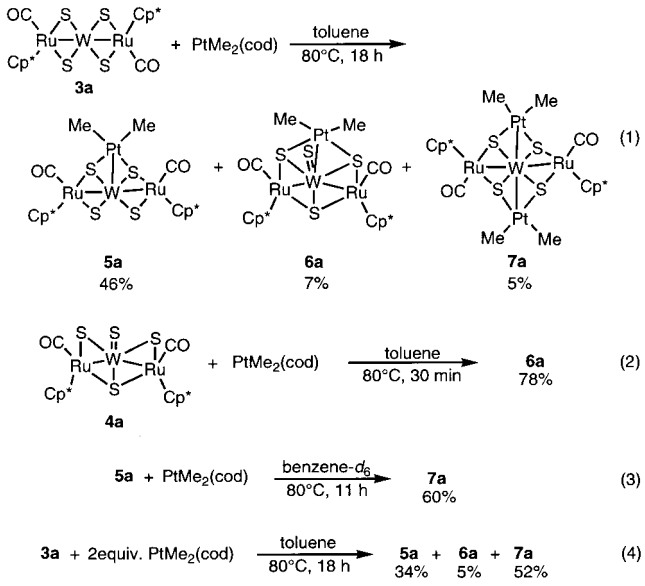

The crystal structure of **5b** was determined by the X-ray crystal structure analysis. Selected bond distances and angles are listed in Table 1. As shown in Figure 1, cluster **5b** contains a WS_4 unit with S−W−S angles of 108.1(2)−112.0(3)° which is bound to a platinum atom by two sulfur atoms and two ruthenium atoms by four sulfur atoms. The W−S distances in the tetrathiotungstate moiety are in the range 2.199(6)−2.252(6) Å. The distances between μ_2-sulfur atoms (S1, S2) and the tungsten atom are 2.210(6) and 2.199(6) Å, respectively, and are nearly the same as those in **3b** (2.214(3)−2.220(3) Å).[5] In contrast, the distances between μ_3-sulfur atoms (S3, S4) and the tungsten atom are 2.252(6) and 2.245(6) Å, respectively, and are elongated to some extent compared with those in **3b**. The elongation of the W−S distances results from further coordination of the sulfur atom to the platinum fragment in the tetrathiotungstate cluster. An elongation similar to this is also observed in **1** (W−(μ_3-S) = 2.268(4), 2.272(3) Å).[5] The platinum atom with two sulfur atoms and two methyl ligands adopts a slightly distorted square planar geometry. The angles of C1−Pt−C2, S3−Pt−C1, C2−Pt−S4,

(5) (a) Yuki, M.; Okazaki, M.; Inomata, S.; Ogino, H. *Organometallics* **1999**, *18*, 3728. (b) Yuki, M.; Okazaki, M.; Inomata, S.; Ogino, H. *Angew. Chem., Int. Ed. Engl.* **1998**, *37*, 2126.

(6) Yuki, M.; Okazaki, M.; Ogino, H. *Chem. Lett.* **1999**, 649.

Table 1. Selected Interatomic Distances (Å) and Bond Angles (deg) for [{(η^5-C_5Me_4Et)Ru(CO)}$_2${W(μ_3-S)$_2$(μ-S)$_2$}(PtMe$_2$)] (5b)

	Distances		
W−Pt	2.777(2)	W−Ru1	2.860(2)
W−Ru2	2.870(2)		
W−S1	2.210(6)	W−S2	2.199(6)
W−S3	2.252(6)	W−S4	2.245(6)
Pt−S3	2.352(6)	Pt−S4	2.364(7)
Ru1−S1	2.404(6)	Ru1−S3	2.370(6)
Ru2−S2	2.391(7)	Ru2−S4	2.386(7)
Pt−C1	2.10(3)	Pt−C2	2.07(3)
	Angles		
Pt−W−Ru1	90.69(5)	Pt−W−Ru2	93.44(6)
Ru1−W−Ru2	175.07(6)		
S1−W−S2	112.0(3)	S1−W−S3	108.1(2)
S1−W−S4	110.3(2)	S2−W−S3	108.9(3)
S2−W−S4	108.1(2)	S3−W−S4	109.3(2)
S1−Ru1−S3	98.3(2)	S2−Ru2−S4	97.8(2)
W−S1−Ru1	76.5(2)	W−S2−Ru2	77.3(2)
W−S3−Pt	74.2(2)	W−S3−Ru1	76.4(2)
W−S4−Pt	74.1(2)	W−S4−Ru2	76.6(2)
Pt−S3−Ru1	116.3(2)	Pt−S4−Ru2	120.0(3)
S3−Pt−C1	87.5(8)	S3−Pt−C2	166.4(8)
S4−Pt−C1	164.1(8)	S4−Pt−C2	88.4(9)
C1−Pt−C2	84(1)	S3−Pt−S4	102.2(2)

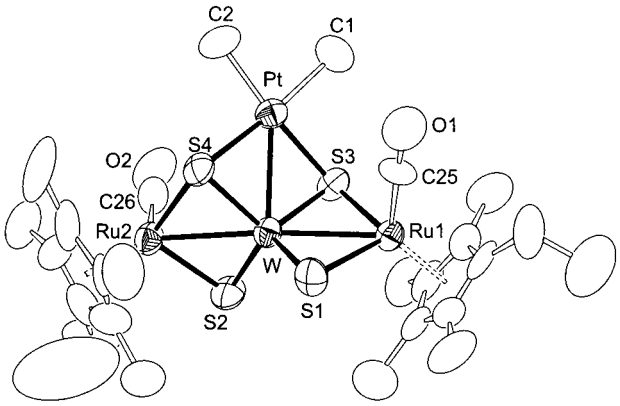

Figure 1. ORTEP drawing of [{(η^5-C_5Me_4Et)Ru(CO)}$_2$-{W(μ_3-S)$_2$(μ-S)$_2$}(PtMe$_2$)] (**5b**) with 50% ellipsoids.

and S3−Pt−S4 are in the range 84(1)−88.4(9)°. The spectroscopic data of **5** are consistent with the crystal structure of **5b**. The ^{1}H NMR spectrum of **5a** shows two singlet signals at 1.61 and 2.49 ppm ($^2J_{H-Pt}$ = 88 Hz) assignable to two chemically equivalent Cp* ligands and two methyl ligands of a PtMe$_2$ fragment, respectively. In the IR spectrum, a CO stretching band appeared only in the terminal CO region (1959 cm^{-1}).

The elemental analysis and mass spectral data of **6a** established the same formula, {Cp*Ru(CO)}$_2$(WS$_4$)-(PtMe$_2$), as **5a**. The spectroscopic features of **6a** resemble those of [{Cp*Ru(CO)}$_2${W(=S)(μ_3-S)$_3$}{W(CO)$_4$}] (**2**)[5] and are consistent with the structure as shown in eqs 1 and 2. The ^{1}H NMR spectrum of **6a** shows two singlet signals at 1.61 and 2.24 ppm ($^2J_{H-Pt}$ = 88 Hz), which are assigned to two chemically equivalent Cp* ligands and two methyl ligands of a PtMe$_2$ fragment, respectively. In the ^{13}C{^{1}H} NMR spectrum, the signals of two carbonyl ligands appeared equivalently at 203.4 ppm. The ^{13}C{^{1}H} signal of the PtMe$_2$ moiety appeared at −11.5 ppm. The chemical shift is characteristic for an alkyl α-carbon bound to the platinum center. In the IR spectrum, a CO stretching band appeared only in the terminal CO region (1984 cm^{-1}).

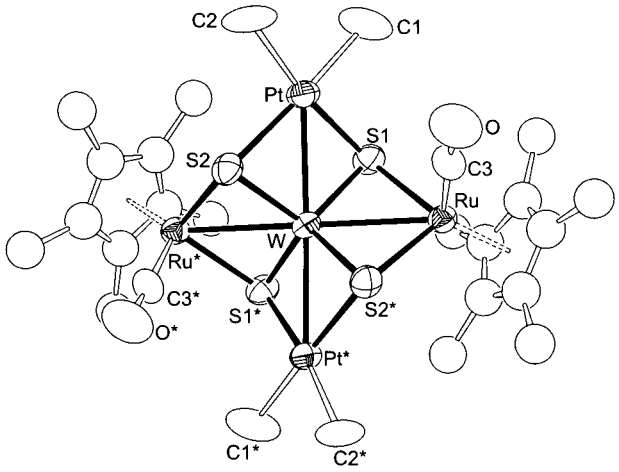

Figure 2. ORTEP drawing of [{Cp*Ru(CO)}$_2${W(μ_3-S)$_4$}-(PtMe$_2$)$_2$] (**7a**) with 50% ellipsoids. The disordered Cp* ligand was omitted for clarity.

Table 2. Selected Interatomic Distances (Å) and Bond Angles (deg) for [{Cp*Ru(CO)}$_2${W(μ_3-S)$_4$}(PtMe$_2$)$_2$] (7a)

	Distances		
W−Pt	2.7835(7)	W−Ru	2.872(2)
W−S1	2.241(5)	W−S2	2.246(5)
Pt−S1	2.350(5)	Pt−S2	2.375(5)
Ru−S1	2.400(5)	Ru−S2*	2.412(5)
Pt−C1	2.07(2)	Pt−C2	2.13(3)
	Angles		
Pt−W−Pt*	169.73(5)	Pt−W−Ru	88.32(3)
Pt−W−Ru*	92.29(3)	Ru−W−Ru*	173.25(7)
S1−W−S2	109.0(2)	S1−W−S1*	111.4(2)
S1−W−S2*	108.6(2)	S1−Ru−S2*	98.4(2)
W−S1−Pt	74.6(1)	W−S1−Ru	76.3(2)
W−S2−Pt	74.0(1)	W−S2−Ru*	76.0(1)
Pt−S1−Ru	112.1(2)	Pt−S2−Ru*	116.9(2)
S1−Pt−C1	85.7(8)	S1−Pt−C2	170.9(7)
S2−Pt−C1	171.5(7)	S2−Pt−C2	87.8(7)
C1−Pt−C2	85(1)	S1−Pt−S2	101.3(2)

The structure of **7a** is unequivocally determined by the X-ray crystal structure analysis (Figure 2). Selected bond distances and angles are listed in Table 2. In cluster **7a**, there is a C_2 symmetry axis on the tungsten atom. The crystal structure exhibits a tetrathiotungstate moiety connecting the two ruthenium fragments Cp*Ru(CO)$_2$ and the two platinum fragments PtMe$_2$. The W−S distances (2.241(5), 2.246(5) Å) are somewhat longer than those in cluster **3b** (2.214(3)−2.220(3) Å).[5] This trend is also observed in clusters **1** and **5b**. Each metal−metal distance (W−Ru = 2.872(2) Å, W−Pt = 2.7835(7) Å) is almost the same as that in **5b** and lies in the normal range expected for each metal−metal single bond.[7] The angles of C1−Pt−C2, S1−Pt−C1, C2−Pt−S2, and S1−Pt−S2 are in the range 85(1)−101.3-(2)°, indicating that each platinum center with two sulfur and two methyl ligands adopts a slightly distorted square planar geometry. Newman projections of **5** and **7** along the Ru−W−Ru axis are depicted in Figure 3.

(7) Chetcuti, M. J. In *Comprehensive Organometallic Chemistry II*; Abel, E. W., Stone, F. G. A., Wilkinson, G., Eds.; Pergamon Press: Oxford, U.K., 1995; Vol. 10, Chapter 2.

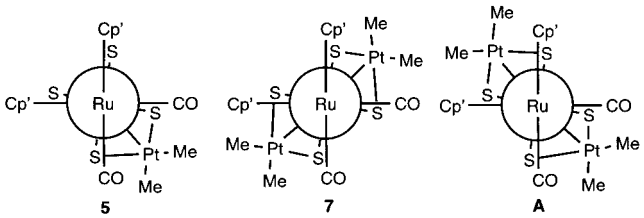

Figure 3. Newman projections of **5**, **7**, and conformer **A**.

In cluster **5**, the $PtMe_2$ fragment occupies the position between the CO ligand on the front ruthenium atom and that on the rear ruthenium atom to minimize the steric interaction between $PtMe_2$, CO, and Cp′ groups. It should be noted that any $PtMe_2$ fragment in **7** does not use the position occupied by the $PtMe_2$ fragment in **5**. If this is the case, cluster **7** must adopt the structure shown as conformer **A**, in which the second $PtMe_2$ fragment occupies the position between two bulky Cp′ ligands. To avoid this severe steric crowding, in the real structure of **7**, each $PtMe_2$ fragment occupies the position between CO and Cp′ ligands. The NMR and IR data of **7** are consistent with the crystal structure of **7b**. In the ^{1}H NMR spectrum of **7a**, the signals of two Cp* ligands appear equivalently at 1.53 ppm. As illustrated in Figure 3, two platinum centers are chemically equivalent and two methyl ligands on one platinum atom are inequivalent. Thus, the signals of four methyl ligands appear as two kinds of singlet signals at 2.28 ($^2J_{H-Pt}$ = 89 Hz) and 2.43 ppm ($^2J_{H-Pt}$ = 85 Hz). The IR spectrum shows a strong-intensity band at 1963 cm^{-1} that is assigned to the terminal carbonyl stretching vibration mode.

Reactions of 5a and 7a with HCl. The reactions of clusters **5a** and **7a** with HCl were examined. Treatment of **5a** with excess HCl afforded the chloromethylplatinum complex [{Cp*Ru(CO)}$_2${W(μ_3-S)$_2$(μ-S)$_2$}(PtClMe)] (**8**) in 83% yield (eq 5). The formula of **8** was established

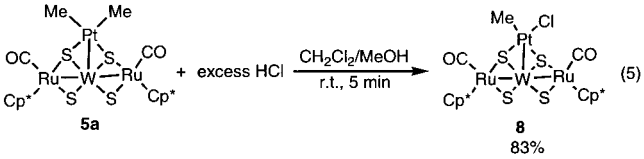

by the elemental analysis and mass spectral data. In the ^{1}H NMR spectrum, the signals of two Cp* ligands appeared inequivalently at 1.51 and 1.52 ppm, which is consistent with the structure illustrated in eq 5. The ^{1}H signal of the PtClMe fragment appears at 2.57 ppm with the ^{195}Pt satellite ($^2J_{H-Pt}$ = 73 Hz). In the reaction of eq 5, further chlorination of the methyl ligand to form [{Cp*Ru(CO)}$_2${W(μ_3-S)$_2$(μ-S)$_2$}(PtCl$_2$)] was not observed. The result is similar to the reaction of [$PtMe_2$(cod)] with excess HCl, which produced [PtClMe(cod)] selectively.[8] The reaction of **7a** with excess HCl proceeded at room temperature to give the bis(chloromethylplatinum) complex [{Cp*Ru(CO)}$_2${W(μ_3-S)$_4$}(PtClMe)$_2$] (**9**) in 70% yield (eq 6). No further chlorination of the methyl ligands in **9** was observed. The formula of **9** was established by the elemental analysis and mass spectral data. The ^{1}H NMR spectrum shows two singlet signals at 1.49 and 2.43 ($^2J_{H-Pt}$ = 73 Hz) ppm, which are

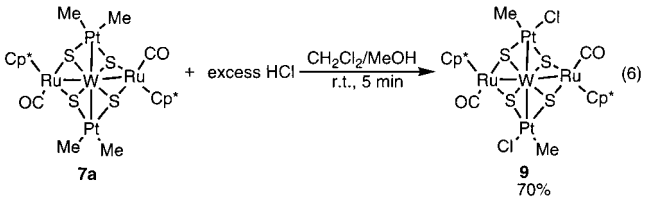

uniquely assigned to two chemically equivalent Cp* ligands on the ruthenium centers and two methyl ligands on the platinum centers, respectively. The reaction of **7a** with 1 equiv of HCl gave almost quantitatively the monochloro derivative [{Cp*Ru(CO)}$_2${W(μ_3-S)$_4$}(PtClMe)(PtMe$_2$)] (**10**) (eq 7). In the ^{1}H NMR

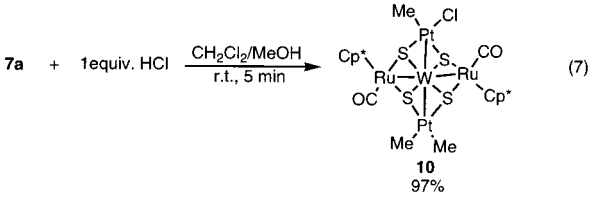

spectrum of **10**, the signals of two Cp* ligands appear inequivalently at 1.60 and 1.41 ppm. The ^{1}H signals of three chemically inequivalent methyl ligands on two platinum centers appear at 2.44 ($^2J_{H-Pt}$ = 74, 85 Hz) and 2.26 ppm ($^2J_{H-Pt}$ = 88 Hz) with a 2:1 intensity ratio. The signal at 2.44 ppm consists of accidentally overlapped signals of the two methyl ligands.

In the reaction of [{Cp*Ru(CO)}$_2${W(μ_3-S)$_4$}(PtMe$_2$)$_2$] (**7a**) with 1 equiv of HCl, monochloro product **10** was formed selectively. This result implies that the chlorination of the methyl ligands on the first platinum center in **7a** effectively reduces the reactivity of the methyl ligands on the second platinum center toward HCl, indicating that the two platinum centers communicate with each other electronically via the tetrathiotungstate ligand. Rauchfuss et al. reported the electronic communication of the tetrathiotungstate cluster [{CpRu(PPh$_3$)}$_2${W(μ-S)$_4$}]. The tetrathiotungstate cluster underwent the substitution reaction of PPh_3 by CO to give the monosubstituted cluster [{CpRu(PPh$_3$)}{CpRu(CO)}{W(μ-S)$_4$}], and further substitution was not observed at all.[9]

Reactions of 3 and 4 with [Pt(C$_2$H$_4$)(PPh$_3$)$_2$]. The trinuclear cluster **3** reacted with 2 equiv of the platinum(0) complex [Pt(C$_2$H$_4$)(PPh$_3$)$_2$] to give cluster **11** (eq 8).

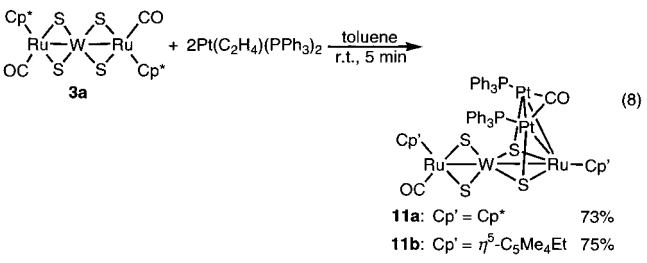

The elemental analysis and mass spectral data of **11** established the formula Cp′$_2$Ru$_2$Pt$_2$WS$_4$(CO)$_2$(PPh$_3$)$_2$, which is formed by elimination of two ethylene and two triphenylphosphine molecules. The structure of **11b** was determined by the X-ray crystal structure analysis

(8) Cook, C. D.; Jauhal, G. S. *J. Am. Chem. Soc.* **1968**, *90*, 1464.

(9) Howard, K. E.; Rauchfuss, T. B.; Wilson, S. R. *Inorg. Chem.* **1988**, *27*, 1710.

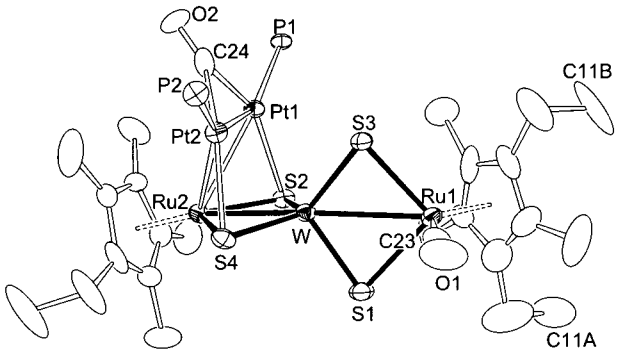

Figure 4. ORTEP drawing of [{(η^5-C_5Me_4Et)Ru(CO)}-{W(μ_3-S)$_2$(μ-S)$_2$}{(η^5-C_5Me_4Et)Ru}{$Pt_2(PPh_3)_2$(μ-CO)}] (**11b**) with 50% thermal ellipsoids. Phenyl groups were omitted for clarity. C11A and C11B denote a disordered ethyl β-carbon atom.

Table 3. Selected Interatomic Distances (Å) and Bond Angles (deg) for [{(η^5-C_5Me_4Et)Ru(CO)}{W(μ_3-S)$_2$(μ-S)$_2$}-{(η^5-C_5Me_4Et)Ru}{$Pt_2(PPh_3)$}$_2$(μ-Co)] (11b)

	Distances		
W−Ru1	2.919(1)	W−Ru2	2.718(1)
Pt1−Ru2	2.826(1)	Pt2−Ru2	2.891(1)
Pt1−Pt2	2.6830(8)		
W···Pt1	3.0401(8)	W···Pt2	2.9532(9)
W−S1	2.239(4)	W−S2	2.275(4)
W−S3	2.240(4)	W−S4	2.285(4)
Pt1−S2	2.409(4)	Pt2−S4	2.392(4)
Ru1−S1	2.391(4)	Ru1−S3	2.391(4)
Ru2−S2	2.357(4)	Ru2−S4	2.359(4)
Pt1−P1	2.248(4)	Pt2−P2	2.257(4)
Pt1−C24	2.01(2)	Pt2−C24	2.03(2)
	Angles		
Ru1−W−Ru2	167.74(4)	Pt2−Pt1−Ru2	63.25(3)
Pt1−Pt2−Ru2	60.78(3)	Pt1−Ru2−Pt2	55.97(3)
Pt1−Ru2−W	66.48(3)	Pt2−Ru2−W	63.45(3)
S1−W−S2	105.5(1)	S1−W−S3	105.0(1)
S1−W−S4	104.7(1)	S2−W−S3	114.3(1)
S2−W−S4	110.6(1)	S3−W−S4	115.6(1)
W−S1−Ru1	78.1(1)	W−S3−Ru1	78.1(1)
W−S2−Ru2	71.8(1)	W−S4−Ru2	71.6(1)
Pt1−S2−W	80.9(1)	Pt1−S2−Ru2	72.7(1)
Pt2−S4−W	78.3(1)	Pt2−S4−Ru2	75.0(1)
Pt2−Pt1−S2	102.18(9)	Pt1−Pt2−S4	103.31(9)
Pt2−Pt1−P1	143.8(1)	Pt1−Pt2−P2	145.7(1)
Pt2−Pt1−C24	48.6(5)	Pt1−Pt2−C24	48.2(5)
Ru2−Pt1−S2	52.81(9)	Ru2−Pt2−S4	51.99(9)
Ru2−Pt1−P1	149.9(1)	Ru2−Pt2−P2	152.1(1)
Ru2−Pt1−C24	96.2(5)	Ru2−Pt2−C24	93.9(5)
S2−Pt1−P1	112.2(1)	S4−Pt2−P2	109.3(1)
S2−Pt1−C24	147.6(5)	S4−Pt2−C24	145.8(5)
P1−Pt1−C24	99.7(5)	P2−Pt2−C24	103.3(5)
Pt1−C24−Pt2	83.3(7)		
S1−Ru1−S3	96.0(1)	S2−Ru2−S4	105.3(1)
Pt1−Ru2−S2	54.49(9)	Pt1−Ru2−S4	100.1(1)
Pt2−Ru2−S2	97.7(1)	Pt2−Ru2−S4	53.05(9)
W−Ru2−S2	52.68(9)	W−Ru2−S4	52.9(1)

(Figure 4). Selected bond distances and angles are listed in Table 3. The molecule contains a tetrathiotungstate fragment in which each of the S1 and S3 atoms bridges one ruthenium and one tungsten atom in a μ_2 fashion, as in the case of **3b**. The S2 and S4 atoms each bridge one tungsten, one ruthenium, and one platinum atom in a μ_3 fashion. The distances of Pt1−Pt2 (2.6830(8) Å), Pt1−Ru2 (2.826(1) Å), and Pt2−Ru2 (2.891(1) Å) are lying in the normal range expected for each metal−metal single bond. The two platinum atoms are bridged by a carbonyl ligand which is originally located on a ruthenium atom in **3b**. The distances of the other two metal−metal bonds (Ru1−W and Ru2−W) are almost the same as those in **3b**.[5] The distances between the tungsten and two μ_3-sulfur atoms (W−S2 = 2.275(4) Å, W−S4 = 2.285(4) Å) are somewhat longer than those of W−S1 (2.239(4) Å) and W−S3 (2.240(4) Å).

The spectroscopic features of **11** are consistent with the crystal structure mentioned above. The IR spectrum of **11a** shows two strong-intensity bands at 1734 and 1946 cm^{-1}, indicating that there exist not only a terminal CO ligand but also a bridging CO ligand. In the ^{1}H NMR spectrum, the signals of two Cp* ligands appear inequivalently at 1.63 and 1.45 ppm. In the ^{31}P-{^{1}H} NMR spectrum, the signals appear at 42.8 and 40.1 ppm as two doublets ($^3J_{P-P}$ = 33 Hz). Furthermore, each ^{31}P signal has two Pt satellites with coupling constants of $^1J_{P-Pt}$ = 5731 and 5722 Hz and $^2J_{P-Pt}$ = 433 and 425 Hz, respectively, apparently showing that cluster **11a** has a platinum−platinum bond.

The reaction of **4a** with [Pt(C_2H_4)(PPh_3)$_2$] in benzene-d_6 was monitored by ^{1}H and ^{31}P NMR spectroscopy. The reaction proceeded immediately at room temperature to give cluster **12** quantitatively (eq 9). Cluster **12** is

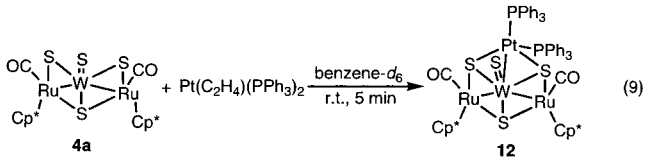

(9)

tentatively assigned to [{Cp*Ru(CO)}$_2${W(=S)(μ_3-S)$_3$}-{Pt(PPh_3)$_2$}], although due to its air sensitivity, isolation of **12** was unsuccessful. In the ^{1}H NMR spectrum of **12**, the signals of two Cp* ligands appear equivalently at 1.73 ppm. The ^{31}P NMR signals of two PPh_3 ligands appear inequivalently at 43.2 and 40.1 ppm as a doublet with the coupling constant $^2J_{P-P}$ = 17 Hz. Two doublet signals have Pt satellites with $^1J_{P-Pt}$ = 2753 and 4774 Hz, respectively. The existence of two chemically inequivalent PPh_3 ligands implies that the platinum moiety Pt(PPh_3)$_2$(μ_3-S)$_2$ adopts a tetrahedral geometry.

The tetrathiometalates MS_4^{2-} (M = Mo, W) have been known to work as bridging ligands for connecting metal fragments. For example, the tetrathiometalates combine CuL (L = Cl, Br, SCN, PPh_3) units to produce a wide variety of clusters.[10] Relatively little has been reported about the tetrathiometalates which have organometallic fragments.[11] Clusters **9** and **11** are the first examples in which a tetrathiotungstate bridges more than three organometallic fragments.

Conclusion

This paper describes the cluster construction by using tetrathiotungstate trinuclear clusters [{Cp′Ru(CO)}$_2$-

(10) Jeannin, Y.; Sécheresse, F.; Bernès, S.; Robert, F. *Inorg. Chim. Acta* **1992**, *198−200*, 493 and references therein.

(11) (a) Howard, K. E.; Rauchfuss, T. B.; Wilson, S. R. *Inorg. Chem.* **1988**, *27*, 3561. (b) Shapley, P. A.; Gebeyehu, Z.; Zhang, N.; Wilson, S. R. *Inorg. Chem.* **1993**, *32*, 5646. (c) Ogo, S.; Suzuki, T.; Isobe, K. *Inorg. Chem.* **1995**, *34*, 1304. (d) Zhuang, B.; Yu, P.; Huang, L.; He, L.; Lu, J. *Polyhedron* **1994** *13*, 125. (e) Evans, W. J.; Ansari, M. A.; Ziller, J. W.; Khan, S. I. *Organometallics* **1995**, *14*, 3. (f) Ruiz, J.; Rodríguez, V.; López, G.; Chaloner, P. A.; Hitchcock, P. B. *J. Organomet. Chem.* **1995**, *493*, 77. (g) Mizobe, Y.; Hosomizu, M.; Kubota, Y.; Hidai, M. *J. Organomet. Chem.* **1996**, *507*, 179.

(WS_4)] (**3** and **4**) as a building block. Reaction of [{Cp′Ru(CO)}$_2${W(μ-S)$_4$}] (**3**) with 1 equiv of the platinum(II) complex [PtMe$_2$(cod)] afforded a Ru_2WPt cluster [{Cp′Ru(CO)}$_2${W(μ_3-S)$_2$(μ-S)$_2$}(PtMe$_2$)] (**5**) as a main product. Reaction of **3** with 2 equiv of [PtMe$_2$(cod)] afforded the Ru_2WPt_2 cluster [{Cp′Ru(CO)}$_2${W(μ_3-S)$_4$}(PtMe$_2$)$_2$] (**7**) as the main product. Furthermore, the isomer of **3** [{Cp′Ru(CO)}$_2${W(=S)(μ_3-S)(μ-S)$_2$}] (**4**) reacted with [PtMe$_2$(cod)], affording an isomer of **5**, [{Cp′Ru(CO)}$_2$-{W(=S)(μ_3-S)$_3$}(PtMe$_2$)] (**6**).

Treatment of **5a** with excess HCl resulted in monochlorination of the methyl ligand in the PtMe$_2$ moiety to give [{Cp*Ru(CO)}$_2${W(μ_3-S)$_2$(μ-S)$_2$}(PtClMe)] (**8**) selectively. In the reaction of **7a** with excess HCl, monochlorination at each platinum center takes place to give [{Cp*Ru(CO)}$_2${W(μ_3-S)$_4$}(PtClMe)$_2$] (**9**). The reaction of **7a** with 1 equiv of HCl gave the monochloro complex [{Cp*Ru(CO)}$_2${W(μ_3-S)$_4$}(PtClMe)(PtMe$_2$)] (**10**) quantitatively. This observation indicates that two platinum centers communicate with each other via the tetrathiotungstate ligand.

The reaction of **3** with 2 equiv of [Pt(C_2H_4)(PPh$_3$)$_2$] afforded the unique pentanuclear cluster [{Cp′Ru(CO)}-(WS$_4$)(Cp′Ru){Pt$_2$(PPh$_3$)$_2$(μ-CO)}] (**11**), in which the tetrathiotungstate bridges the mononuclear fragment Cp′Ru(CO) and the three-membered metallacycle (Cp′-Ru){Pt(PPh$_3$)}$_2$(μ-CO).

Experimental Section

General Information and Materials. Infrared spectra were recorded on a Horiba FT-200 spectrometer. ^{1}H, ^{13}C, and ^{31}P NMR spectra were recorded on a Bruker ARX-300 instrument. Mass spectra were obtained on a JEOL-HX110 instrument operating in the fast atom bombardment (FAB) mode. All reactions were performed under a nitrogen atmosphere using deoxygenated solvents dried with appropriate reagents. Acetyl chloride was distilled from phosphorus pentoxide. The clusters [{Cp*Ru(CO)}$_2${W(μ-S)$_4$}] (**3a**), [{Cp*Ru(CO)}$_2$-{W(=S)(μ_3-S)(μ-S)$_2$}] (**4a**), and the C_5Me_4Et derivatives **3b** and **4b** were synthesized according to the published procedures.[5] The complexes [PtMe$_2$(cod)] (cod = 1,5-cyclooctadiene)[12] and [Pt(C_2H_4)(PPh$_3$)$_2$][8] were prepared by the literature methods.

Reaction of [{Cp*Ru(CO)}$_2${W(μ-S)$_4$}] (3a) with 1 Equiv of [PtMe$_2$(cod)]. A Pyrex tube was charged with **3a** (100 mg, 0.119 mmol) and [PtMe$_2$(cod)] (43 mg, 0.130 mmol), and toluene (5 mL) was introduced into this tube under high vacuum by the trap-to-trap-transfer technique. The tube was flame-sealed and heated at 80 °C for 18 h. After the mixture was cooled, the tube was unsealed in the air. Volatiles were removed under reduced pressure, and the residue was charged on a silica gel flash column. Elution with toluene−hexane (1:1) mixture gave a dark red eluate. Concentration of the fraction under high vacuum afforded [{Cp*Ru(CO)}$_2${W(μ_3-S)$_4$}(PtMe$_2$)$_2$] (**7a**; 8 mg, 5%). Further elution with toluene gave an orange band, a red band, and a green band in that order. Concentration of the fractions afforded **3a** (9 mg, 10%), [{Cp*Ru(CO)}$_2$-{W(μ_3-S)$_2$(μ-S)$_2$}(PtMe$_2$)] (**5a**; 58 mg, 46%) and [{Cp*Ru(CO)}$_2$-{W(=S)(μ_3-S)$_3$}(PtMe$_2$)] (**6a**; 10 mg, 7%), respectively. Analytically pure samples of **5a**, **6a**, and **7a** were obtained by recrystallization from a dichloromethane−hexane mixture at room temperature. Data for **5a** are as follows. ^{1}H NMR (300 MHz, C_6D_6): δ 2.49 (s, 6H, $^2J_{H-Pt}$ = 88 Hz, PtMe$_2$), 1.61 (s, 30H, Cp*). ^{13}C{^{1}H} NMR (75.5 MHz, C_6D_6): δ 202.7 (CO), 100.0 (C_5Me_5), 10.4 (C_5Me_5), −9.5 (PtMe$_2$). IR (KBr): 1959 cm^{-1} (ν(CO)). FAB MS (Xe, *m*-nitrobenzyl alcohol matrix): *m*/*z* 1052 (M$^+$ − Me). Anal. Calcd for $C_{24}H_{36}O_2PtRu_2S_4W$: C, 27.05; H, 3.40. Found: C, 27.17; H 3.29. Data for **6a** are as follows. ^{1}H NMR (300 MHz, C_6D_6): δ 2.24 (s, 6H, $^2J_{H-Pt}$ = 88 Hz, PtMe$_2$), 1.61 (s, 30H, Cp*). ^{13}C{^{1}H} NMR (75.5 MHz, C_6D_6): δ 203.4 (CO), 98.4 (C_5Me_5), 10.0 (C_5Me_5), −11.5 (PtMe$_2$). IR (KBr): 1984 cm^{-1} (ν(CO)). FAB MS (Xe, *m*-nitrobenzyl alcohol matrix): *m*/*z* 1052 (M$^+$ − Me). Anal. Calcd for $C_{24}H_{36}O_2PtRu_2S_4W$: C, 27.05; H, 3.40. Found: C, 26.93; H 3.54. Data for **7a** are as follows. ^{1}H NMR (300 MHz, C_6D_6): δ 2.43 (s, 6H, $^2J_{H-Pt}$ = 85 Hz, PtMe$_2$), 2.28 (s, 6H, $^2J_{H-Pt}$ = 89 Hz, PtMe$_2$), 1.53 (s, 30H, Cp*). ^{13}C{^{1}H} NMR (75.5 MHz, C_6D_6): δ 201.5 (CO), 100.8 (C_5-Me$_5$), 10.9 (C_5Me_5), −6.4, −7.0 (PtMe$_2$). IR (KBr): 1963 cm^{-1} (ν(CO)). FAB MS (Xe, *m*-nitrobenzyl alcohol matrix): *m*/*z* 1176 (M$^+$ − 2Me − 2CO). Anal. Calcd for $C_{26}H_{42}O_2Pt_2Ru_2S_4W$: C, 24.19; H, 3.28. Found: C, 23.75; H 3.38.

Reaction of [{Cp′Ru(CO)}$_2${W(=S)(μ_3-S)(μ-S)$_2$}] (4) with [PtMe$_2$(cod)]. A Pyrex tube was charged with [{Cp*Ru(CO)}$_2$-{W(=S)(μ_3-S)(μ-S)$_2$}] (**4a**; 150 mg, 0.178 mmol) and [PtMe$_2$-(cod)] (68 mg, 0.203 mmol), and toluene (5 mL) was introduced into this tube under high vacuum by the trap-to-trap-transfer technique. The tube was flame-sealed and heated at 80 °C for 30 min. After cooling, the tube was unsealed in the air. Removal of volatiles under reduced pressure and recrystallization of the residue from a dichloromethane−hexane mixture at room temperature afforded dark green crystals of [{Cp*Ru-(CO)}$_2${W(=S)(μ_3-S)$_3$}(PtMe$_2$)] (**6a**; 148 mg, 78%) in an analytically pure form. The C_5Me_4Et derivative of **6a**, [{(η^5-C_5Me_4-Et)Ru(CO)}$_2${W(=S)(μ_3-S)$_3$}(PtMe$_2$)] (**6b**), was also obtained in 73% yield by starting from [{(η^5-C_5Me_4Et)Ru(CO)}$_2${W(=S)-(μ_3-S)(μ-S)$_2$}] (**4b**) in a similar procedure. Data for **6b** are as follows. ^{1}H NMR (300 MHz, C_6D_6): δ 2.25 (q, 4H, $^3J_{H-H}$ = 8 Hz, CH_2CH$_3$), 2.24 (s, 6H, $^2J_{H-Pt}$ = 88 Hz, PtMe$_2$), 1.69, 1.66, 1.64, 1.60 (s, 24H, C_5Me_4Et), 0.79 (t, 6H, $^3J_{H-H}$ = 8 Hz, CH$_2$CH_3). ^{13}C{^{1}H} NMR (75.5 MHz, C_6D_6): δ 203.2 (CO), 101.3, 99.3, 99.2, 98.8, 98.4 (C_5Me_4Et), 19.1 (CH$_2$), 14.8, 10.0, 9.84, 9.76, 9.73 (*Me*), −11.4 (PtMe$_2$). IR (KBr): 1981 cm^{-1} (ν(CO)). Anal. Calcd for $C_{24}H_{36}O_2PtRu_2S_4W$: C, 28.55; H, 3.69. Found: C, 28.46; H 3.74.

Reaction of [{Cp′Ru(CO)}$_2${W(μ-S)$_4$}] (3) with 2 Equiv of [PtMe$_2$(cod)]. A Pyrex tube was charged with **3a** (163 mg, 0.194 mmol) and [PtMe$_2$(cod)] (151 mg, 0.453 mmol), and toluene (5 mL) was introduced into this tube under high vacuum by the trap-to-trap-transfer technique. The tube was flame-sealed and heated at 80 °C for 18 h. After cooling, the tube was unsealed in the air. Isolation of **5a** (70 mg, 34%), **6a** (10 mg, 5%), and **7a** (129 mg, 52%) was achieved by a procedure similar to that in the reaction of [{Cp*Ru(CO)}$_2$-{W(μ-S)$_4$}] (**3a**) with 1 equiv of [PtMe$_2$(cod)]. The C_5Me_4Et derivatives [{(η^5-C_5Me_4Et)Ru(CO)}$_2${W(μ_3-S)$_2$(μ-S)$_2$}(PtMe$_2$)] (**5b**), **6b**, and [{(η^5-C_5Me_4Et)Ru(CO)}$_2${W(μ_3-S)$_4$}(PtMe$_2$)$_2$] (**7b**) were also obtained in 49%, 6%, and 34% yields, respectively, from **3b** by a similar procedure. Data for **5b** are as follows. ^{1}H NMR (300 MHz, C_6D_6): δ 2.50 (s, 6H, $^2J_{H-Pt}$ = 87 Hz, PtMe$_2$), 2.2 (m, 4H, CH_2CH$_3$), 1.67 (s, 12H, C_5Me_4Et), 1.60 (s, 6H, C_5Me_4Et), 1.59 (s, 6H, C_5Me_4Et), 0.79 (t, J = 8 Hz, 6H, CH$_2$CH_3). ^{13}C NMR (75 MHz, C_6D_6): δ 202.8 (CO), 103.2, 101.03, 101.01, 100.6, 100.4 (C_5Me_4Et), 19.8 (CH$_2$), 15.3, 10.54, 10.49, 10.44, 10.3 (*Me*), −9.2 (PtMe$_2$). IR (KBr): 1956 cm^{-1} (ν(CO)). Anal. Calcd for $C_{26}H_{40}O_2PtRu_2S_4W$: C, 28.55; H, 3.69. Found: C, 29.04; H, 3.85. Data for **7b** are as follows. ^{1}H NMR (300 MHz, C_6D_6): δ 2.45 (s, 6H, $^2J_{H-Pt}$ = 83 Hz, PtMe$_2$), 2.29 (s, 6H, $^2J_{H-Pt}$ = 89 Hz, PtMe$_2$), 2.15 (m, 4H, CH_2CH$_3$), 1.61 (s, 6H, C_5Me_4Et), 1.57 (s, 6H, C_5Me_4Et), 1.52 (s, 12H, C_5Me_4Et), 0.70 (t, J = 8 Hz, 6H, CH$_2$CH_3). ^{13}C{^{1}H} NMR (75.5 MHz, C_6D_6): δ 201.3 (CO), 103.4, 101.62, 101.61, 101.59, 100.9 (C_5-Me$_4$Et), 19.7 (CH$_2$), 14.7, 10.81, 10.80, 10.79, 10.4 (*Me*), −6.3, −6.9 (PtMe$_2$). IR (KBr): 1992, 1975 cm^{-1} (ν(CO)). FAB MS (Xe, *m*-nitrobenzyl alcohol matrix): *m*/*z* 1305 (M$^+$ − Me). Anal. Calcd for $C_{28}H_{46}O_2Pt_2Ru_2S_4W$: C, 25.50; H, 3.51. Found: C, 25.63; H, 3.29.

(12) Clark, H. C.; Manzer, L. E. *J. Organomet. Chem.* **1973**, *59*, 411.

Table 4. Summary of Crystallographic Parameters

	5b	**7a**	**11b**·CH_2Cl_2
formula	$C_{26}H_{40}O_2PtRu_2S_4W$	$C_{26}H_{42}O_2Pt_2Ru_2S_4W$	$C_{61}H_{66}O_2Cl_2P_2Pt_2Ru_2S_4W$
fw	1093.93	1291.02	1868.46
a, Å	16.458(10)	15.069(9)	11.382(2)
b, Å	26.13(1)	15.529(7)	12.783(3)
c, Å	15.661(4)	16.542(7)	22.341(5)
α, deg	90	90	89.36(2)
β, deg	90	95.69(4)	82.45(2)
γ, deg	90	90	71.52(1)
V, Å^3	6736(4)	3851(3)	3054(1)
space group	*Pbca*	*C*2/*c*	$P\bar{1}$
Z	8	4	2
d_{calcd}, g cm^{-3}	2.16	2.23	2.03
cryst size, mm	0.45 × 0.30 × 0.25	0.50 × 0.50 × 0.50	0.20 × 0.20 × 0.50
μ(Mo Kα), cm^{-1}	86.81	111.90	72.25
transmissn factor range	1.00−0.74	1.00−0.51	1.00−0.70
2θ range, deg	3−55	3−60	3−55
scan mode	ω	$\omega-2\theta$	$\omega-2\theta$
ω-scan width, deg	1.2 + 0.35 tan θ	1.1 + 0.35 tan θ	1.25 + 0.35 tan θ
ω-scan rate, deg min^{-1}	4.0	4.0	8.0
T, K	293	293	150
no. of unique data collected	7731	5622	14 012
no. of data used	3480 ($I > 2\sigma(I)$)	3038 ($I > 3\sigma(I)$)	10995 ($I > 3\sigma(I)$)
no. of params refined	325	92	679
final *R*	0.059	0.059	0.051
final R_w	0.082	0.099	0.079
final GOF	1.00	1.16	3.85
largest shift/esd in final cycle	0.37	0.04	2.27
max resid electron dens, e Å^{-3}	1.36	2.72	2.52

Reaction of 5a with [PtMe$_2$(cod)]. A Pyrex NMR tube (5 mm o.d.) was charged with **5a** (5.2 mg, 4.9 μmol) and [PtMe$_2$(cod)] (2.1 mg, 6.3 μmol), and benzene-d_6 (0.4 mL) was introduced into this tube under high vacuum by the trap-to-trap-transfer technique. The tube was flame-sealed and heated to 80 °C. The reaction was monitored by ^{1}H NMR spectroscopy. In the course of the reaction, the signals of **7a** appeared, while those of **5a** decreased. After 11 h, the ^{1}H NMR spectrum showed that **5a** was transformed to **7a** in 60% conversion yield, where 26% of **5a** and 50% of the starting [PtMe$_2$(cod)] remained intact.

Reaction of 5a with Excess HCl. HCl was prepared in situ by the reaction of acetyl chloride with methanol.[8] To a dichloromethane−methanol (5:2, 7 mL) solution of **5a** (115 mg, 0.108 mmol) was added acetyl chloride (250 mg, 3.18 mmol) with stirring. Volatiles were removed under reduced pressure. Recrystallization of the residue from dichloromethane−hexane afforded [{Cp*Ru(CO)}$_2${W(μ_3-S)$_2$(μ-S)$_2$}(PtClMe)] (**8**; 97 mg, 83%) as red crystals. Spectroscopic data for **8** are as follows. ^{1}H NMR (300 MHz, C_6D_6): δ 2.57 (s, 3H, $^2J_{H-Pt}$ = 73 Hz, PtClMe), 1.52 (s, 15H, Cp*), 1.51 (s, 15H, Cp*). IR (KBr): 1965 cm^{-1} (ν(CO)). FAB MS (Xe, *m*-nitrobenzyl alcohol matrix): *m*/*z* 1015 (39, M$^+$ − 2CO − Me − H). Anal. Calcd for $C_{23}H_{33}O_2ClPtRu_2S_4W$: C, 25.43; H, 3.06. Found: C, 25.57; H, 3.06.

Reaction of 7a with Excess HCl. To a dichloromethane−methanol (3:1, 2 mL) solution of **7a** (14 mg, 11 μmol) was added acetyl chloride (36 mg, 454 μmol) with stirring. Volatiles were removed under reduced pressure. Recrystallization of the residue from dichloromethane−hexane afforded [{Cp*Ru(CO)}$_2${W(μ_3-S)$_4$}(PtClMe)$_2$] (**9**; 10 mg, 70%) as red crystals. Data for **9** are as follows. ^{1}H NMR (300 MHz, C_6D_6): δ 2.43 (s, $^2J_{H-Pt}$ = 73 Hz, 6H, PtClMe), 1.49 (s, 30H, Cp*). IR (KBr): 1975 cm^{-1} (ν(CO)). FAB MS (Xe, *m*-nitrobenzyl alcohol matrix): *m*/*z* 1225 (M$^+$ − 2CO − Me − Cl − H). Anal. Calcd for $C_{24}H_{36}O_2Cl_2Pt_2Ru_2S_4W$: C, 21.64; H, 2.72. Found: C, 22.26; H, 2.67.

Reaction of 7a with 1 Equiv of HCl. To a dichloromethane−methanol (10:1, 11 mL) solution of **7a** (77 mg, 60 μmol) was added acetyl chloride (4.5 mg, 57 μmol) with vigorous stirring. The volatiles were removed under reduced pressure. Recrystallization of the residue from dichloromethane−hexane afforded [{Cp*Ru(CO)}$_2${W(μ_3-S)$_4$}(PtMe$_2$)(PtClMe)] (**10**; 73 mg, 97%) as red crystals. Data for **10**: ^{1}H NMR (300 MHz, C_6D_6) δ 2.44 (s, $^2J_{H-Pt}$ = 74 Hz, 3H, Pt−Me), 2.44 (s, $^2J_{H-Pt}$ = 85 Hz, 3H, Pt−Me), 2.26 (s, $^2J_{H-Pt}$ = 88 Hz, 3H, Pt−Me), 1.60 (s, 15H, Cp*), 1.41 (s, 15H, Cp*). IR (KBr) 1973 cm^{-1} (ν(CO)). FAB MS (Xe, *m*-nitrobenzyl alcohol matrix): *m*/*z* 1172 (M$^+$ − 2CO − 3Me − Cl − 4H). Anal. Calcd for $C_{25}H_{39}O_2ClPt_2Ru_2S_4W$: C, 22.90; H, 3.00. Found: C, 22.72; H, 2.87.

Reaction of 3a with [Pt(C$_2$H$_4$)(PPh$_3$)$_2$]. A toluene (5 mL) solution of **3a** (49 mg, 58 μmol) and [Pt(C$_2$H$_4$)(PPh$_3$)$_2$] (100 mg, 134 μmol) was stirred at room temperature for 5 min. Volatiles were removed under reduced pressure, and the residue was charged on a silica gel column. Elution with toluene gave a dark brown band. Concentration of the fraction afforded [{Cp*Ru(CO)}(WS$_4$)(Cp*Ru){Pt$_2$(PPh$_3$)$_2$(μ-CO)}] (**11a**; 75 mg, 73%) as a brown powder. Analytically pure crystals were obtained by recrystallization from dichloromethane−hexane at room temperature. The C_5Me_4Et derivative **11b** was also obtained from the reaction of **3b** with [Pt(C$_2$H$_4$)(PPh$_3$)$_2$] by a similar procedure. Data for **11a** are as follows. ^{1}H NMR (300 MHz, C_6D_6): δ 8.1−8.0 (m, 6H, Ph), 8.0−7.9 (m, 6H, Ph), 7.2−7.0 (m, 18 H, Ph), 1.63 (s, 15H, Cp*), 1.45 (s, 15H, Cp*). ^{1}H NMR (300 MHz, CD_2Cl_2): δ 7.7−7.5 (m, 12H, Ph), 7.4−7.2 (m, 18H, Ph), 1.57 (s, 30H, Cp*). ^{13}C NMR (75 MHz, CD_2Cl_2): δ 203.6 (CO), 136.8 (d, J_{C-P} = 5 Hz), 136.2 (d, J_{C-P} = 5 Hz), 134.6 (d, J_{C-P} = 13 Hz), 134.0 (d, J_{C-P} = 13 Hz), 129.9 (d, J_{C-P} = 2 Hz), 129.8 (d, J_{C-P} = 2 Hz), 128.3 (d, J_{C-P} = 10 Hz), 128.2 (d, J_{C-P} = 10 Hz), 100.4 (C_5Me_5), 91.1 (C_5Me_5), 12.0 ($C_5\mathit{Me}_5$), 10.3 ($C_5\mathit{Me}_5$). ^{31}P NMR (121 MHz, CD_2Cl_2): δ 42.8 (d, $^3J_{P-P}$ = 33 Hz, $^1J_{P-Pt}$ = 5731 Hz, $^2J_{P-Pt}$ = 433 Hz, PPh$_3$), 40.1 (d, $^3J_{P-P}$ = 33 Hz, $^1J_{P-Pt}$ = 5772 Hz, $^2J_{P-Pt}$ = 425 Hz, PPh$_3$). IR (KBr): 1946, 1734 cm^{-1} (ν(CO)). FAB MS (Xe, *m*-nitrobenzyl alcohol): *m*/*z* 1700 (M$^+$ − 2CO). Anal. Calcd for $C_{58}H_{60}O_2P_2Pt_2Ru_2S_4W$: C, 39.68; H, 3.45. Found: C, 39.92; H, 3.71. Data for **11b** are as follows. ^{1}H NMR (300 MHz, C_6D_6): δ 8.1−8.0 (m, 6H, Ph), 8.0−7.9 (m, 6H, Ph), 7.2−7.0 (m, 18 H, Ph), 2.19 (q, 2H, $^3J_{H-H}$ = 8 Hz, CH_2), 2.02 (m, 2H, CH_2), 1.67, 1.66, 1.65, 1.64, 1.551, 1.550, 1.37, 1.34 (s, 3Hx8, $C_5\mathit{Me}_4Et$), 0.755 (t, 3H, $^3J_{H-H}$ = 8 Hz, $CH_2C\mathit{H}_3$), 0.746 (t, 3H, $^3J_{H-H}$ = 8 Hz, $CH_2C\mathit{H}_3$). ^{13}C NMR (75 MHz, CD_2Cl_2): δ 203.5 (CO), 136.54 (d, J_{C-P} = 47 Hz), 136.48 (d, J_{C-P} = 47 Hz), 134.6 (d, J_{C-P} = 13 Hz), 134.0 (d, J_{C-P} = 13 Hz), 129.9 (d, J_{C-P} = 2 Hz), 129.8 (d, J_{C-P} = 2 Hz), 128.3 (d, J_{C-P} = 10 Hz), 128.2 (d, J_{C-P} = 10 Hz) (Ph),

103.9, 101.6, 101.1, 100.5, 99.7, 95.7, 91.3, 91.2, 90.8 (C_5Me_4-Et), 20.8, 19.5 (CH_2), 15.0, 12.02, 11.95, 11.8, 10.2, 10.0, 9.91, 9.88 (*Me*). ^{31}P NMR (121 MHz, C_6D_6): δ 41.1 (d, $^3J_{P-P}$ = 33 Hz), 38.2 (d, $^3J_{P-P}$ = 33 Hz). IR (KBr): 1946, 1734 cm^{-1} (ν(CO)). FAB MS (Xe, *m*-nitrobenzyl alcohol): *m*/*z* 1728 ($M^+ - 2CO$). Anal. Calcd for $C_{60}H_{64}O_2P_2Pt_2Ru_2S_4W$: C, 40.41; H, 3.62. Found: C, 40.16; H, 3.62.

Reaction of 4a with [Pt(C$_2$H$_4$)(PPh$_3$)$_2$]. To a benzene-d_6 (0.4 mL) solution of **4a** (3.28 mg, 3.90 μmol) was added [Pt-(C_2H_4)(PPh_3)$_2$] (3.09 mg, 4.13 μmol). The color of the solution immediately turned from orange to reddish brown. After 5 min, the ^{1}H NMR spectrum showed almost quantitative formation of [{Cp*Ru(CO)}$_2${W(=S)(μ_3-S)$_3$}{Pt(PPh_3)$_2$}] (**12**). Purification of **12** was unsuccessful due to its air sensitivity, resulting in decomposition to give the starting material **4a** and unidentified precipitates. Spectroscopic data for **12** are as follows. ^{1}H NMR (300 MHz, C_6D_6): δ 8.3−8.2 (m, 6H, Ph), 7.6−7.5 (m, 6H, Ph), 7.0−6.8 (m, 18 H, Ph), 1.73 (s, 30H, Cp*). ^{31}P NMR (121 MHz, C_6D_6): δ 43.2 (d, $^2J_{P-P}$ = 17 Hz, $^1J_{P-Pt}$ = 2753 Hz, PPh_3), 40.1 (d, $^2J_{P-P}$ = 17 Hz, $^1J_{P-Pt}$ = 4774 Hz, PPh_3). IR (KBr): 1956 cm^{-1} (νCO).

X-ray Crystallography. Single crystals of **5b**, **7a**, and **11b**·CH_2Cl_2 were grown from a dichloromethane−hexane mixture at −30 °C. Crystallographic data are summarized in Table 4. The crystals were mounted on glass fibers. Diffraction measurements were carried out on a Rigaku AFC-6S or AFC-5R diffractometer using graphite-monochromated Mo Kα radiation (λ = 0.710 73 Å). All reflections were corrected for Lorentz−polarization and absorption effects. Absorption corrections were made by the ψ-scan method; maximum and minimum transmission factors are shown in Table 4. Lattice parameters were determined from 25 reflections with 2θ angles in the range 25−30°. The space groups were identified on the basis of systematic absences and confirmed by successfully solving the crystal structures. Structures were solved by Patterson methods (PATTY) (**5b** and **11b**·CH_2Cl_2) or by direct methods (SIR92) (**7a**). The disordered Cp* ligand of **7a** was treated as a rigid group to which isotropic thermal factors were applied. The dichloromethane solvate in **11b**·CH_2Cl_2 was refined isotropically. All other non-hydrogen atoms were refined anisotropically. Hydrogen atoms were not located. In the structure of **11b**·CH_2Cl_2, the occupancies of the disordered ethyl β-carbon atom in one C_5Me_4Et ligand (C11A and C11B) were determined to give similar equivalent temperature factors and were fixed in least-squares refinements. Data reduction and refinement were performed using teXsan software packages. Selected interatomic distances and bond angles for compounds **5b**, **7a**, and **11b** are listed in Tables 1−3, respectively.

Supporting Information Available: Text, tables, and figures giving X-ray crystallographic data for crystals of **5b**, **7a**, and **11b**·CH_2Cl_2. This material is available free of charge via the Internet at http://pubs.acs.org.

OM000985T